ICANS-XIII
13th Meeting of the International Collaboration on
Advanced Neutron Sources
October 11-14, 1995
Paul Scherrer Institut, 5232 Villigen PSI, Switzerland

TIME COLLIMATION FOR ELASTIC NEUTRON SCATTERING AT A PULSED SOURCE

V.L.Aksenov and Yu.V. Nikitenko

Frank Laboratory of Neutron Physics, JINR, 141980 Dubna, Moscow Region, Russia

ABSTRACT

Conditions for carrying out elastic neutron scattering experiments using the time-of-flight technique are considered. It is shown, that the employment of time dependent neutron beam collimation in the source-sample flight path increases the luminosity of the spectrometer under certain resolution restrictions. Time collimation modes are proposed for small-angle scattering and neutron reflection.

Introduction

A traditional design of the elastic neutron scattering spectrometer (Fig.1) implies angle collimation of the neutron beam on the source-sample flight path and detection of neutrons scattered at different angles. For fixed neutron wavelengths, which is the case for a steady-state neutron source, the dependence of the scattering cross-section on the q scattering vector is measured at a definite q resolution. At a pulsed neutron source, a wide range of neutron wavelengths is used, thus, making it possible to measure the scattering cross-section over an interval of scattering vector values an order of magnitude greater than at a steady-state source. At the same time, however, conditions of measurements on the scattering vector interval differ greatly. This implies that the ratio of the value for distortions of the scattering law (the scattering cross-section) to the statistical precision in measuring the scattering law greatly depends on the scattering vector. This, in fact, may be considered equal to a narrowing of the measuring interval with a given reliability.

At the same time, at pulsed neutron sources, the possibility exists of changing the neutron phase volume on the sample with time in the interval between power pulses of the neutron

source. In the present paper we propose changing the solid angle at which the neutron source is visible and the cross-section of the neutron beam on the sample with time (starting from the moment of initiation of the source pulse) following certain laws. This will be considered for three types of spectrometers: the small-angle diffusion scattering spectrometer, the small-angle diffractometer and the reflectometer.

2. Optimization criteria

We shall consider the optimization criteria at length for the small-angle scattering spectrometer. Figure 2 presents the scheme of the small-angle scattering spectrometer with axial geometry. The main functional elements of the spectrometer are: the first and the second diaphragms used for angle collimation of the incident beam, placed at distances of L_0 and $L_0+ L_1$, respectively, from the source; the sample position (made coincident with the second diaphragm) and scattered neutron detector placed at a distance $L_0+L_1+L_2$ from the neutron source. The dependence of the scattering cross-section $d\sigma(q)/d\Omega$ (the scattering law is $F(q)$) on the scattering vector $q = 4\pi\sin(\theta/2)/\lambda$ is measured with the spectrometer, where λ is the neutron wavelength and θ is the scattering angle. For the intensity of the scattered beam, $J(\lambda,q)$, and the root-mean-square deviation, $\sigma_q(\lambda)$, the following relationships apply [1]:

$$J(\lambda,q) = j_0(\lambda)\, R_1^2R_2^2F(q)R\Delta R/L_1^2/L_2^2,$$
$$\sigma_q(\lambda) = \pi/\lambda((R_1/L_1)^2+R_2^2(1/L_1+1/L_2)^2+(\Delta R/L_2)^2/3+(R/L_2)^2(\Delta\lambda/\lambda)^2/3)^{1/2}, \quad (1)$$

where $j_0(\lambda)$ is the neutron flux before the first diaphragm, R_1 and R_2 are the radii of the first and second diaphragms, respectively, R and ΔR are the radius and width of the detecting element in the detector and $\Delta\lambda$ is the wavelength uncertainty.

The well-known approach in optimization [1,2] involves the achievement of maximum intensity at fixed values for the root-mean-square deviation of the scattering vector, the scattering vector itself, neutron wavelength and total flight path, $L_1+ L_2$. This can be attained if the following relationships are satisfied [2]:

$$L_1 = L_2\,,\ R_1 = 2R_2 = (2/3)^{1/2}\Delta R = (2/3)^{1/2}R\Delta\lambda/\lambda. \quad (2)$$

Conditions should be stated, however, appropriate for the whole interval of scattering vector values. It is apparent that the scattering intensity should be represented in relation to the scattering vector [3]:

$$J = \int j_0(q)\ \Phi(q)\ dq, \quad (3)$$

where $j_0(q)$ is the scattering intensity at a definite value of q and unit value of scattering law, $\Phi(q)=\int F(q')R(q,q')dq'$ is the scattering law distorted by the resolution of scattering vector;

R(q,q') is the resolution function. For $j_0(q)$ and R(q,q') the following relationships should be satisfied:

$$j_0(q) = q \int j_s(\lambda)d\lambda \quad \text{and} \quad R(q,q') = \int R(q,q',\lambda)\, j_s(\lambda)\, d\lambda \,/\, \int j_s(\lambda)d\lambda, \qquad (4)$$

where $j_s(\lambda) = \lambda^2 R_1^2 R_2^2 j_0(\lambda)$, $R(q,q',\lambda)$ - resolution function at a definite value of λ, $\lambda_{max}=2R_{max}/qL_2$, $\lambda_{min}=2R_{min}/qL_2$ are the integration limits, R_{max} and R_{min} are the maximal and minimal radii of the detecting area of the detector.

We introduce a deviation of the scattering law $\delta F(q) = |(\Phi(q) - F(q))|$ and a root-mean-square deviation of the scattering law $\delta F_{st}(q)$, caused by the statistics of counting scattered neutrons. Now we can write the optimization conditions as follows:

$$A = \int \delta F(q) \,/\, F(q)\, dq = \text{const}$$

$$B = \int (\delta F_{st}(q) \,/\, \delta F(q))^2\, dq = \int (F(q)/\delta F(q)^2/(j_0(q)F(q))dq = \min \qquad (5)$$

Additional conditions are the fixed neutron spectrum and fixed wavelength interval, as well as measuring time, total neutron flight path and detector size. The relationship between the flight paths, $a=L_1/L_2$, and the relationship between the radii of the diaphragms in relation to time, starting from the moment of initiation of the pulse, $b(t)=R_1(t)/R_2(t)$, should be determined. Since the time of neutron flight from the source to the diaphragm is directly proportional to the neutron wavelength, b(t) can be transformed to $b(\lambda)$.

3. Diffusion small-angle scattering

The resolution function in a certain approximation may be represented by a Gaussian [3] with a variance of the scattering vector, $D_q(q)$:

$$D_q(q) = \int \sigma_q^{-1}(\lambda) j_s(\lambda) d\lambda \,/\, \int \sigma_q^{-3}(\lambda) j_s(\lambda) d\lambda. \qquad (6)$$

In this case in the first approximation for the distortion of the scattering law, we obtain $\delta F(q) = 1/2 dF^2(q)/dq^2 D_q(q)$. Then we choose the approximations $\Delta R = 0$ and $\Delta\lambda = 0$, at which $\delta\sigma_q(\lambda)$ is inversely proportional to the neutron wavelength and it is possible under certain conditions to obtain an analytical solution. This takes place in practice and is realised for the case of high luminosity, when the resolution is determined only by the sizes of the neutron source and the sample. Let us next represent the diaphragm radii as $R_1 = R_{10}(\lambda/\lambda_{min})^n$ and $R_2 = R_{20}(\lambda/\lambda_{min})^n$. The problem can be formulated as follows: optimal values of the a,b and n parameters should be determined so that conditions (5) are fulfilled. To this end the equation $dB/dX = 0$, where X = a,b,n, should be satisfied. This gives us a=1 and b=2.

To determine the optimal value of the n parameter, numerical calculations should be made. Figure 3 presents the results of these calculations. When carrying out the calculations, the Maxwellian spectrum with a characteristic wavelength λ_t = 1.8 A was taken. The following parameter values were chosen: $L_1 = L_2$ = 40m, R_{min} = 5cm and R_{max} = 50cm. The wavelength interval 0.5 - 10A corresponds a scattering vector interval 0.0008 - 0.16A^{-1}. The dependence of parameter $\eta(n) = B(n=0)/B(n)$ for different scattering laws is given in Fig.3. From this figure we notice that for the 1/q law (curve 1) the maximum for $\eta(n)$ is achieved at n = -0.98. For the $\exp(-pq^2)$ law the maximum for $\eta(n)$ is at positive values of the n parameter (curves 2 and 3). As an illustration, Fig.4 shows the dependence $\delta F_{st}^2(q)/\delta F^2(q)$ for the scattering law $F(q) = \exp(-100(A^2)q^2)$ for n=0 and n=1/4. One can see that the curve 2 (n=1/4) runs integrally below curve 1 (n=0). We also notice that at large q the statisticaling accuracy decreases.

4. Neutron reflection

Figure 5 presents the scheme of the reflectometer. The neutron beam is incident on the sample at the θ angle of slide. Two diaphragms, placed in the ZX plane at distances L_1 and L_2 from the source, are used to collimate the beam. Suppose that in the X-axis direction the diaphragm sizes are considerably greater than in the Z-axis direction. Then for the variance of the scattering vector (reflection vector) we have ($\Delta\lambda$ is assumed to be 0):

$$D_q(q)= k^2 \cos^2(\theta)(z_1^2+ z_2^2)/3L_0^2, \qquad (7)$$

where k is the wave vector, z_1 and z_2 are the diaphragm sizes in the direction of the Z-axis, $L_0 = L_2 - L_1$.

The following relation holds for $j_0(q)$:

$$j_0(q) = j_0(\lambda)z_1(\lambda)x_1z_2(\lambda)x_2/ L_0^2/q^2 \quad , \qquad (8)$$

where x_1 and x_2 are the diaphragm sizes in the direction of the X-axis. Let us represent z_1 and z_2 as $z_1 = z_2 = z_0 (\lambda/\lambda_{min})^n$. Figure 6 gives the $\eta(n)$ dependence for different scattering laws at the angle of reflection θ = 6 mrad and wavelength interval 0.7 - 10A. It can be seen that, as in the case of the small-angle spectrometer, the optimal n value may be either positive or negative depending on the type of scattering law.

5. Small-angle diffraction

Let us consider the case of small-angle powder diffractometry. In this connection we choose a diffractometer scheme identical to the scheme for small-angle diffusion scattering

(Fig.2). Depending on the scattering vector, the scattering law for the Bragg diffraction, as is well-known, is a delta-function. Therefore, the employment of conditions (5) presents difficulties. Because of this, let us formulate a simplified (though universally used) criteria:

$$C = \int \delta q(q)/q \, dq = \text{const} \quad \text{and} \quad E = \int j_0(q)\Phi(q)dq = \max \qquad (9)$$

The dependence $\delta q(q)/q$ for different values of the n parameter is given in Fig.7. Compared to the case when n = 0, at n = 1 $\delta q/q$ increases at small q and decreases at large q. At n = -1 the pattern of the $\delta q/q$ behaviour, compared to the case when n = 0, appears to be the reverse. From this it follows that if a higher resolution of reflexes at small (large) q is required, it is more preferable to use the power law of diaphragm radius variation with an exponent of n = -1 (n = 1). Figure 8 presents the dependence of the $\eta = E(n)/E(n = 0)$ parameter for the scattering law $F(q) = \sum_\tau \delta(q-q_\tau)$, where q_1=7.94E-04, q_2=8.16E-04, q_3=8.7E-4, q_4=1.0E-03, q_5=1.35E-03, q_6=2.2E-03, q_7=4.345E-03, q_8=9.7E-03, q_9=2.31E-02, q_{10} =5.65E-02. It is apparent that negative values of the n parameter are the most optimal for the ten reflexes given.

6. Conclusion

In the present paper the time-of-flight mode of neutron beam collimation on the source-sample flight path is considered. The calculations show that at a fixed distortion of the scattering law and following certain collimation laws, the statistical accuracy of measurements increases many-fold. The proposed operating regime for the elastic scattering spectrometers is rather simple to realise. Its use is the most effective at low-frequency pulsed sources where a broad wavelength interval is available. This method makes it possible to form an optimal (according to neutron wavelength) phase volume on the sample and it is suitable for both hot and cold neutron sources.

7. Acknowledgements

The authors are grateful to L. Cser and B.N. Savenko for usefull discussions and to T.V. Prikhodko and A. Shaeffer for preparing the English translation of this report.

8. References

[1] R.W. Hendricks, *J. Appl. Cryst.* 11 (1978) 15
[2] D.F.R. Mildner, J.M. Carpenter, *J. Appl. Cryst.* 17 (1984) 249
[3] D.F.R. Mildner, J.M. Carpenter and D.L. Worcester, *J. Appl. Cryst.* 19 (1986) 311.

$$V_{phase} = d^3p \times d^3r \propto \Omega \times S_{beam} / \lambda^3$$

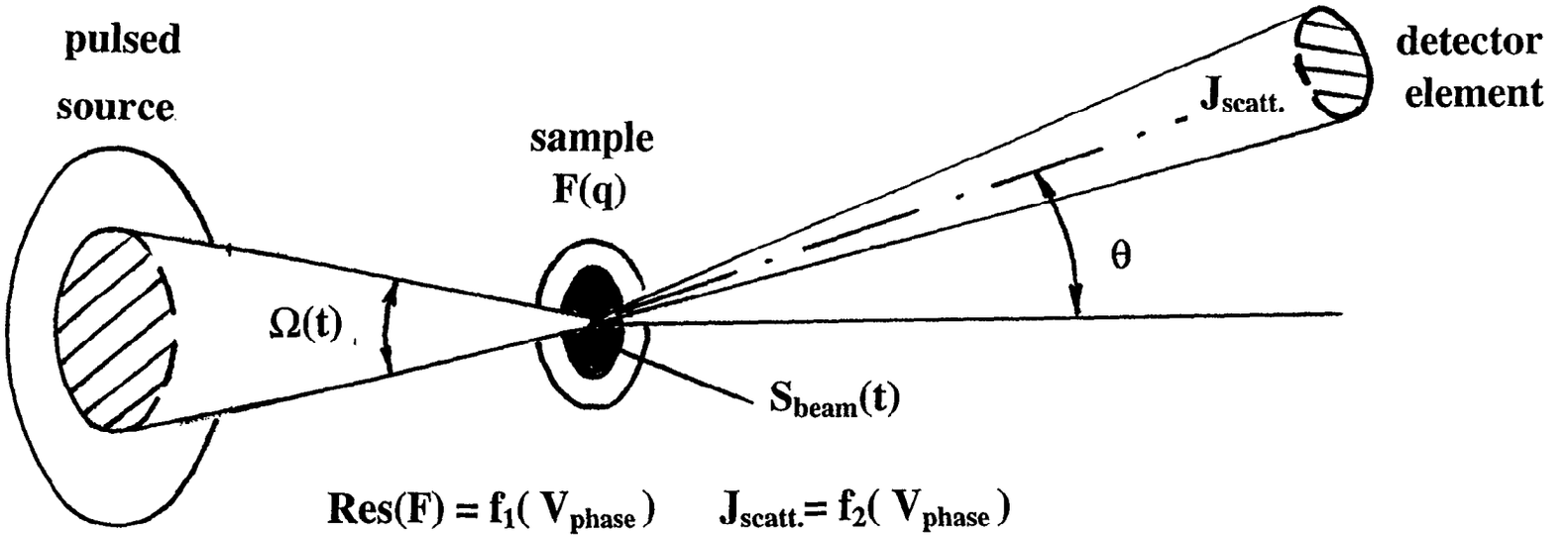

$$Res(F) = f_1(V_{phase}) \qquad J_{scatt.} = f_2(V_{phase})$$

$$V_{phase} \times \lambda^3 = f(t \propto \lambda)$$

Fig. 1. Layout of the elastic scattering neutron spectrometer with a time-of-flight collimation of the neutron beam;

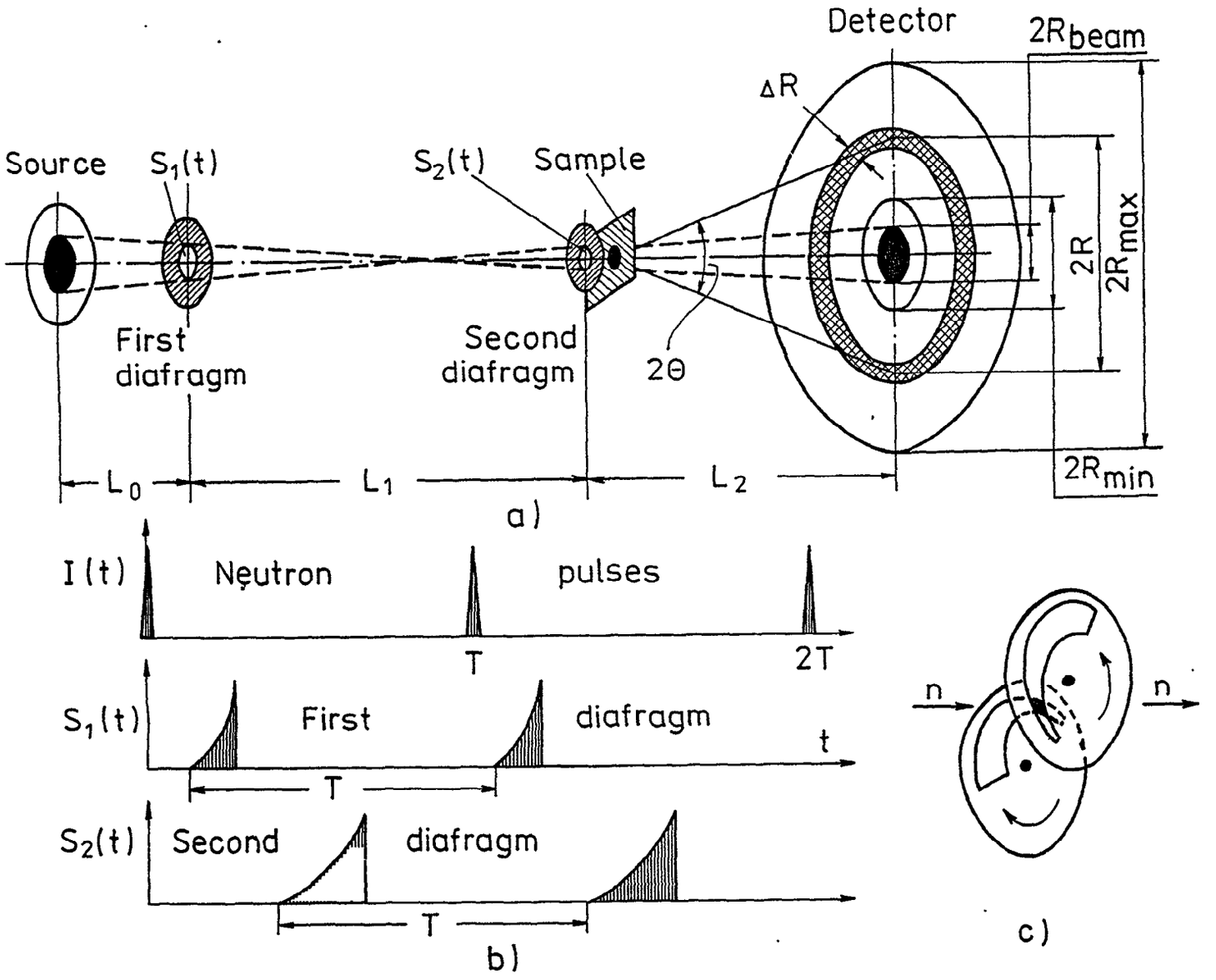

Fig. 2. a) Scheme of the small-angle neutron scattering spectrometer with a time-of-flight collimation of the neutron beam: two diaphragms on the flight path to the sample have an area of S1(t) and S2(t) which change with time starting from the moment of initiation of the source pulse;

b) time diagram which explains the operation of the spectrometer for the period T of recurring power pulses of the neutron source;

c) a possible version of the diaphragm design in the form of two disks made of absorbing neutron material, rotating at the frequency of the power pulses. Slots in the disks meet in mutually perpendicular directions;

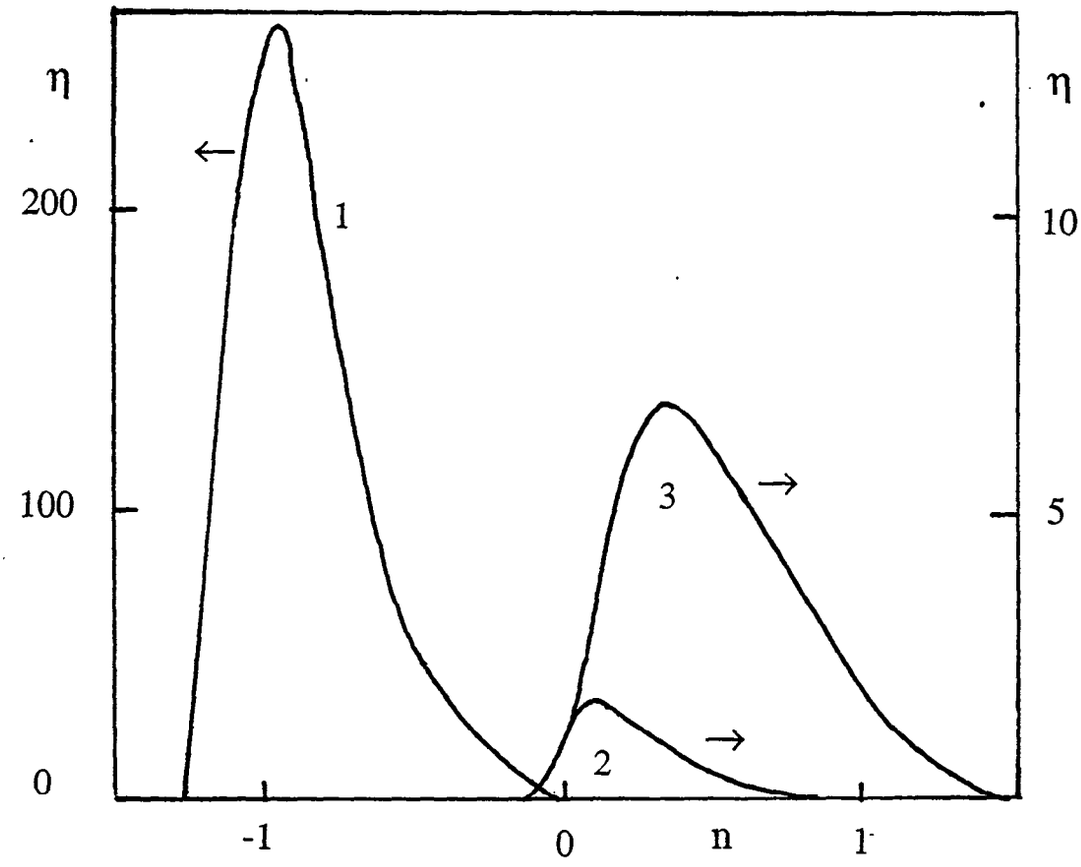

Fig. 3. Dependence of the η(n) parameter for different small-angle diffusion neutron scattering laws: F(q) = 1/q - curve 1; F(q) = exp(-pq^2) and p=10A^2 - curve 2, p=100A^2- curve 3;

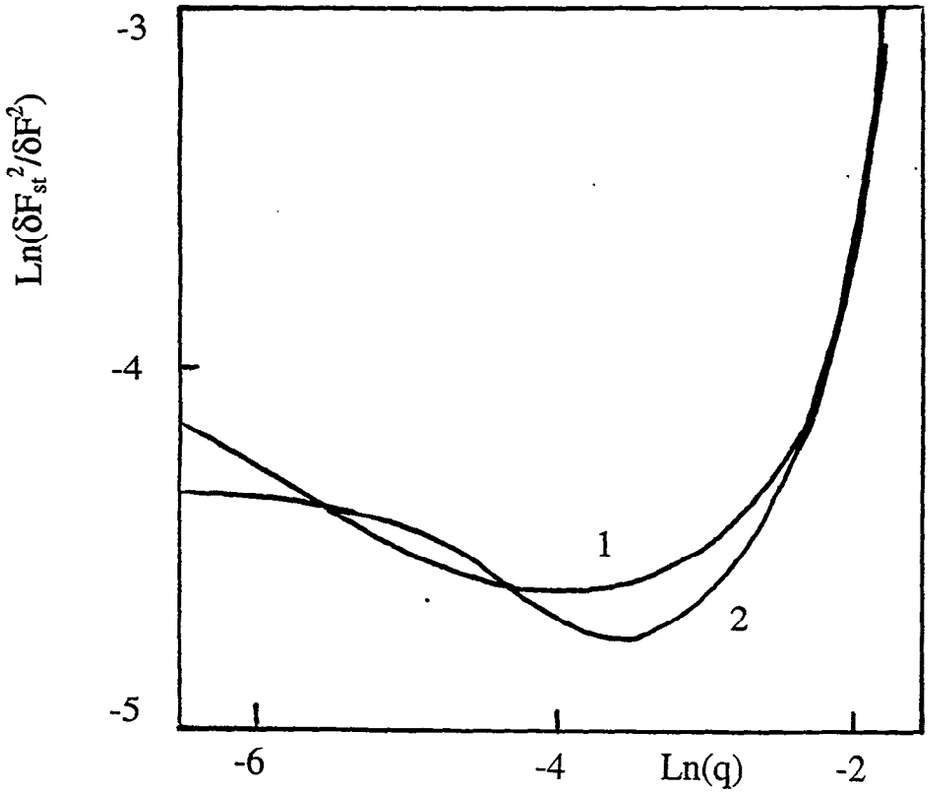

Fig. 4. Dependence of δF^2$_{st}$(q)/δF^2(q) for the scattering law F(q) = exp(-100q^2) at different values for the n parameter: 1- n=0; 2 - n=1/4;

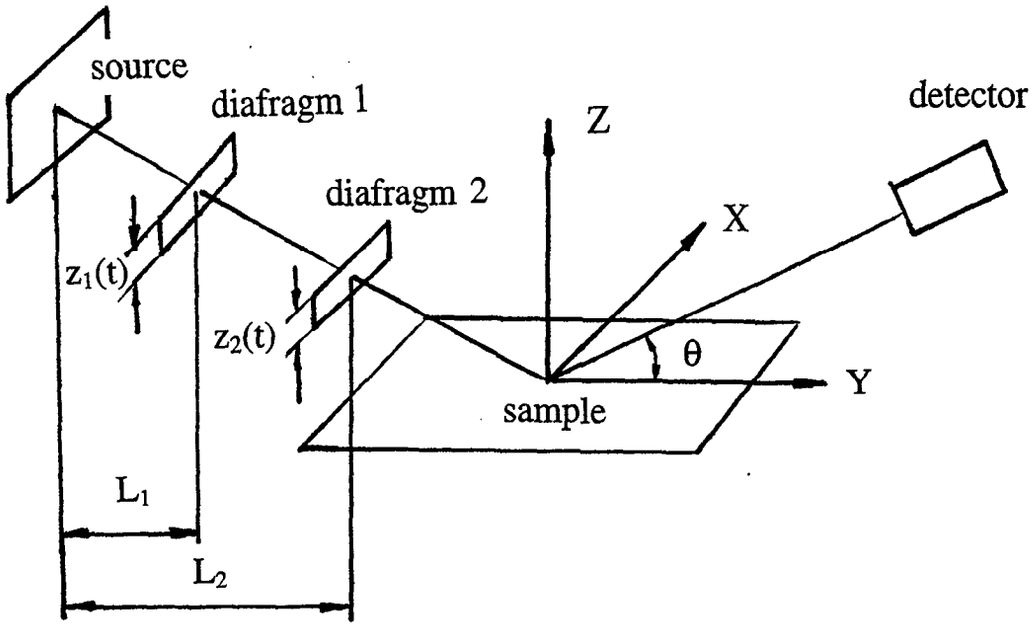

Fig. 5. Neutron reflectometer with a time-of-flight collimation of the neutron beam;

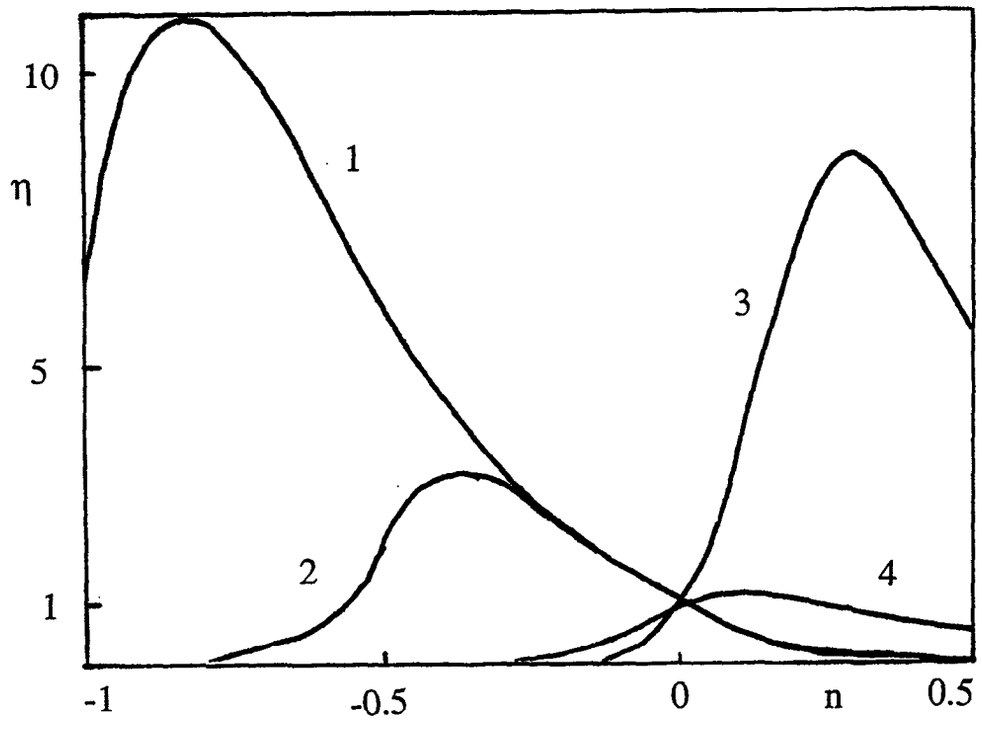

Fig. 6. Dependence of the η(n) parameter for different neutron reflection laws: $F(q) = q^{-4}$ - curve 1; $F(q) = q^{-1}$ - curve 2; $F(q) = \exp(-rq)$ and r = 50 A - curve 3, r = 100 A - curve 4;

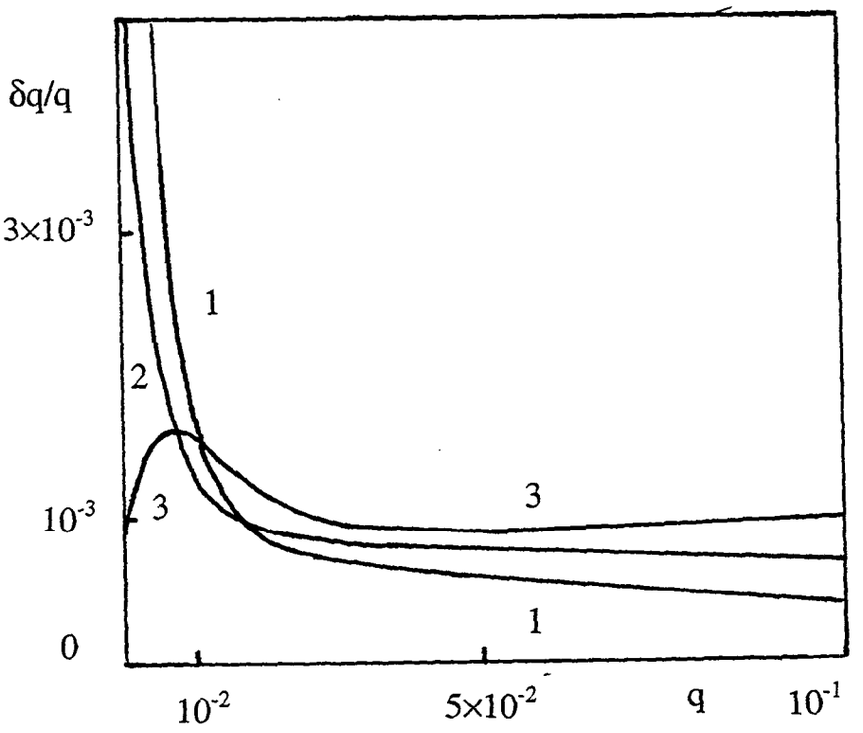

Fig. 7. Dependence of $\delta q(q)/q$ at different values of the n parameter: 1- n=1, 2 - n=0, 3 - n=-1;

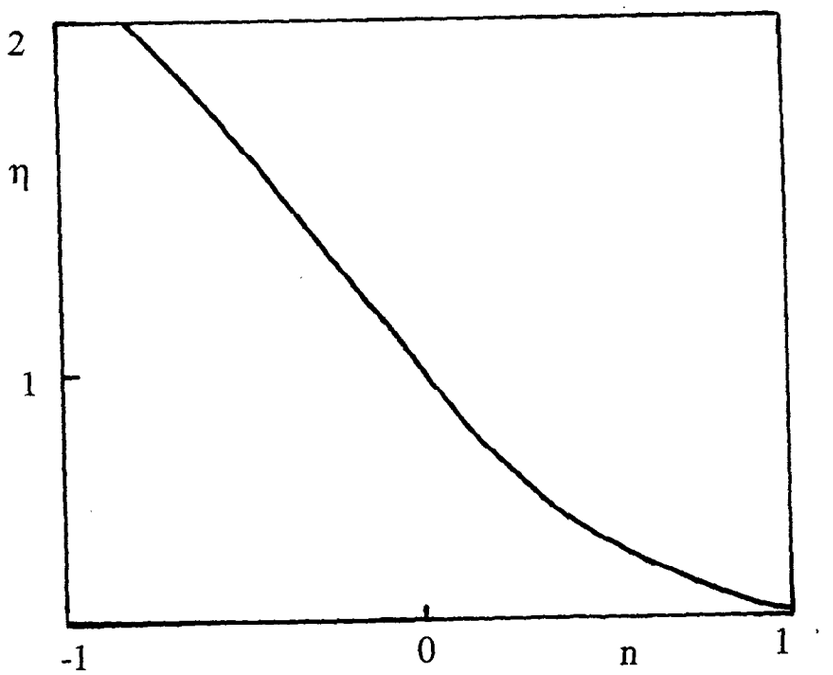

Fig. 8. Dependence of the $\eta=E(n)/E(n=0)$ parameter for the case of ten reflexes in the Bragg neutron diffraction.